Proceedings of the
Annual Stability Conference
Structural Stability Research Council
Atlanta, Georgia, April 22-24, 2026

Fastener-based inelastic analysis of steel deck diaphragms using the instantaneous center method

Firaol Fekadu[1], Hyeyoung Koh[2]

Abstract

The Instantaneous Center Method (ICM) is a nonlinear, mechanics-based approach used in AISC 360 to evaluate steel connection behavior and has recently been extended to estimate the shear strength of bare steel deck diaphragms by modeling inelastic load–deformation behavior of individual fasteners, including arc-spot welds and screws. Compared to traditional elastic analysis methods, the ICM provides a more realistic representation of diaphragm behavior by explicitly capturing nonlinear force redistribution and connector deformation. However, prior diaphragm applications of the ICM exhibited systematic overprediction of shear capacity relative to experimental results, largely due to the use of simplified fastener load–deformation models.

This study develops refined load–deformation models for arc-spot welds and screws based on digitized experimental data from the literature, incorporating key geometric and material parameters such as effective weld diameter, screw diameter, and deck thickness. These refined fastener models are implemented within the ICM framework to predict diaphragm shear strength. Predicted capacities are compared against experimental results, AISI S100 provisions, and prior ICM predictions that relied on idealized fastener behavior. Results demonstrate that incorporating refined fastener models significantly improves the accuracy of ICM-based shear strength predictions and reduces previously observed overestimation trends. By better representing fastener-level inelastic behavior, the ICM framework with refined fastener load–deformation curves enhances the ability to capture nonlinear force transfer mechanisms governing diaphragm response. This improvement strengthens the applicability of the ICM for evaluating steel diaphragm strength and contributes toward more reliable assessment of diaphragm performance and structural stability.

1. Introduction

Steel deck diaphragms are a critical component of lateral force–resisting systems in structural steel buildings, providing in-plane shear transfer through a combination of deck geometry and mechanical fasteners. Current diaphragm design practice is based on elastic analysis procedures, in which diaphragm strength is assumed to be governed by the elastic capacity of the most highly loaded

[1]Graduate Research Assistant, Washington State University, Pullman, WA, <firaol.fekadu@wsu.edu>
[2]Assistant Professor, Washington State University, Pullman, WA, <hyeyoung.koh@wsu.edu>

fastener. While such approaches are used due to their simplicity and generally conservative nature at the design level from elastic analysis, they do not explicitly account for nonlinear fastener behavior or post-elastic force redistribution that occurs prior to ultimate diaphragm failure. To address these limitations, Koh et al. (2025) extended the Instantaneous Center Method (ICM), which was developed for bolted and welded steel connections (Crawford and Kulak 1971; Brandt 1982) and used in AISC 360 Chapter 7 for steel connection design, to assess shear strength of bare steel deck diaphragms. By incorporating the inelastic load–deformation behavior of individual fasteners within the ICM framework, force redistribution resulting from fastener softening is captured through the movement of the instantaneous center of rotation in response to changes in relative fastener stiffness.

Koh et al. (2025) demonstrated the feasibility of applying the ICM to bare steel deck diaphragms incorporating arc-spot welds and screws and established an accessible computational framework for diaphragm analysis using the ICM. However, the ICM-based diaphragm shear strength predictions have shown a tendency toward overestimation of diaphragm shear capacity when compared with experimental results. Koh et al. (2025) used generalized fastener load–deformation backbone curves obtained from the literature: (1) Arc-spot weld response which was idealized using a simplified trilinear representation based on available experimental data reported by Snow and Easterling (2008) and (2) screw behavior which was modeled using a generalized load–deformation relationship proposed by Moen et al. (2014). In these representations, fastener responses were not differentiated with respect to variations in fastener geometry or deck thickness.

Prior studies have emphasized the importance of fastener load–deformation behavior in the response of cold-formed steel (CFS) systems and steel deck diaphragms. Finite element modeling of screw-fastened CFS connections has shown that connection stiffness and force–displacement response vary with sheet thickness and are strongly influenced by contact conditions between the screw and steel plies (Kalo and K. Peterman 2020). Fastener-based nonlinear modeling approaches have been used to evaluate the lateral response of CFS shear walls by explicitly incorporating connector load–deformation relationships, showing that connector behavior strongly influences overall strength and deformation response (Derveni, Gerasimidis, and K. D. Peterman 2020). Experimental investigations on steel deck side-lap and structural connectors have shown that fastener strength and stiffness vary with connection geometry, fastener configuration, and deck thickness, and that experimentally derived backbone curves can be used to represent connector behavior in analytical models (Torabian and Schafer 2021). Collectively, these studies highlight the importance of representing fastener load–deformation behavior in a way that reflects connection-specific characteristics, providing motivation for mechanics-based analysis frameworks that can incorporate nonlinear connector response when evaluating steel deck diaphragm strength.

The objective of this study is to extend the applicability of the ICM for bare steel deck diaphragms and enhance its accuracy and reliability through refined fastener load–deformation models. Digitized experimental data for arc-spot welds and side-lap screws were used to construct backbone curves that explicitly incorporate key geometric and material parameters, such as effective weld diameter, screw diameter, and deck thickness. These refined fastener models were integrated within the existing ICM framework (Koh et al. 2025) to evaluate diaphragm shear strength. Predicted diaphragm capacities were compared with experimental results reported in the Steel Deck Institute

Diaphragm Design Manual (SDI DDM) (Luttrell 2006), data from the Steel Diaphragm Innovation Initiative (SDII) database (O'Brien 2017), elastic design provisions in AISI S100 (2016), and ICM predictions based on idealized fastener load-deformation relationships. The comparisons demonstrate that improved representation of fastener-level inelastic behavior significantly reduces overprediction trends and thus enhances the reliability of ICM-based diaphragm strength estimates.

2. Instantaneous Center Method

The instantaneous center method (ICM) assesses the inelastic strength of fastener groups within bare steel deck diaphragms. The ICM determines equilibrium by relating the nonlinear load–deformation behavior of individual fasteners to a rigid-body rotation about a trial instantaneous center of rotation. The ICM computes the equilibrium of a fastener group by iteratively locating the point about which the group rotates as a rigid body. The analysis begins by assigning coordinates to each fastener and selecting an initial trial location for the instantaneous center of rotation, typically at the geometric centroid of the group. The diaphragm is assumed to rotate as a rigid body about this point, and the deformation in each fastener is calculated based on its radial distance from the instantaneous center. The fastener farthest from the instantaneous center experiences the maximum deformation, corresponding to the limit deformation defined by its backbone curve, while other fasteners deform proportionally to their relative distance. In the present study, the resisting force in each fastener is obtained from its calculated deformation using the refined fastener-specific load–deformation relationships.

The diaphragm configuration is illustrated in Figure 1, where L denotes diaphragm length, L_s denotes joist spacing, w denotes diaphragm width, and P denotes external unit load. This study considered two configurations: (1) diaphragms with arc-spot welds at interior, edge, and end supports and sheet-to-sheet screws at side-lap connections, which is consistent with common diaphragm construction and (2) diaphragms with only arc-spot welds. In the present implementation of the ICM for bare steel deck diaphragms, fastener-based diaphragm strength is evaluated assuming connector-controlled limit states. While earlier diaphragm-level ICM applications employed generalized fastener load–deformation representations derived from experimental data, this study adopts fastener-specific backbone curves directly obtained from experiments, enabling a more detailed representation of nonlinear stiffness degradation and post-peak behavior.

2.1 Refined Load–Deformation Models of Fasteners

2.1.1 Sheet-to-Sheet Screws

The load–deformation relationships of sheet-to-sheet screw fasteners were adopted from the monotonic backbone models developed by Tao et al. (2016) for single-shear screw-fastened connections, covering a range of fastener diameters (#8, #10, and #12) and ply thickness combinations (18 to 97 mil). This study incorporated only the monotonic steel-to-steel data as these most closely represent the loading conditions associated with diaphragm shear testing and strength evaluation. Unlike the previous study (Koh et al. 2025) that employed a single load–deformation equation for #10 screws (Moen et al. 2014), this study directly utilizes the tabulated backbone parameters reported by Tao et al. (2016). This approach allows each diaphragm configuration to be paired with the specific screw diameter and sheet thickness combination corresponding to the tested specimen, thereby

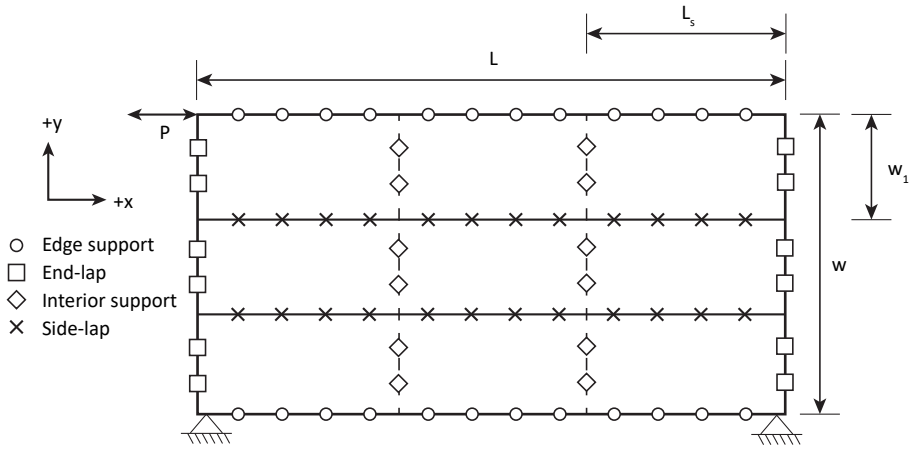

Figure 1: Representative diaphragm layout showing end, edge, interior, and side-lap fasteners used in the ICM analysis.

improving the physical relevance and accuracy of the fastener model.

Each screw load–deformation backbone follows a four-region piecewise format consisting of elastic, strain-hardening, post-peak softening, and residual response regions (Figure 2). The screw force–deformation response is evaluated piecewise using the tabulated parameters as shown in Eq. 1:

$$F(\delta_i) = \begin{cases} K_e\,\delta_i, & 0 < \delta_i \leq \delta_y, \\ F_y + K_s(\delta_i - \delta_y), & \delta_y < \delta_i \leq \delta_c, \\ F_c + K_c(\delta_i - \delta_c), & \delta_c < \delta_i \leq \delta_r, \\ F_r + K_r(\delta_i - \delta_r), & \delta_r < \delta_i \leq \delta_f \end{cases} \tag{1}$$

where δ_i denotes the deformation of an individual screw fastener, K_e is elastic stiffness, K_s is hardening stiffness, K_c is post-peak softening stiffness, K_r is residual stiffness, δ_y is displacement at the upper limit of the elastic region, δ_c is the displacement at peak load, δ_r is the displacement marking the onset of residual response, δ_f is the displacement at the end of the backbone curve, F_y is the screw force at the end of the elastic region, F_c is the peak load, F_r is at the onset of the residual response, and F_f is at the end of the backbone curve. The parameters are directly extracted from the monotonic backbone tables provided by Tao et al. (2016). The adopted backbone curves represent the experimentally observed screw force–deformation response, including elastic behavior, peak strength, and post-peak degradation measured in monotonic steel-to-steel tests.

This piecewise formulation is applied using the experimentally derived backbone parameters, ensuring consistency with the experimentally derived backbones. For each fastener in the diaphragm model, the appropriate parameter set is selected based on its diameter and the sheet-thickness combination of the specimen being simulated. This implementation enables the ICM to represent realistic screw behavior, including nonlinear stiffness reduction and post-peak strength loss, thereby improving its ability to capture force redistribution within fastener groups during inelastic

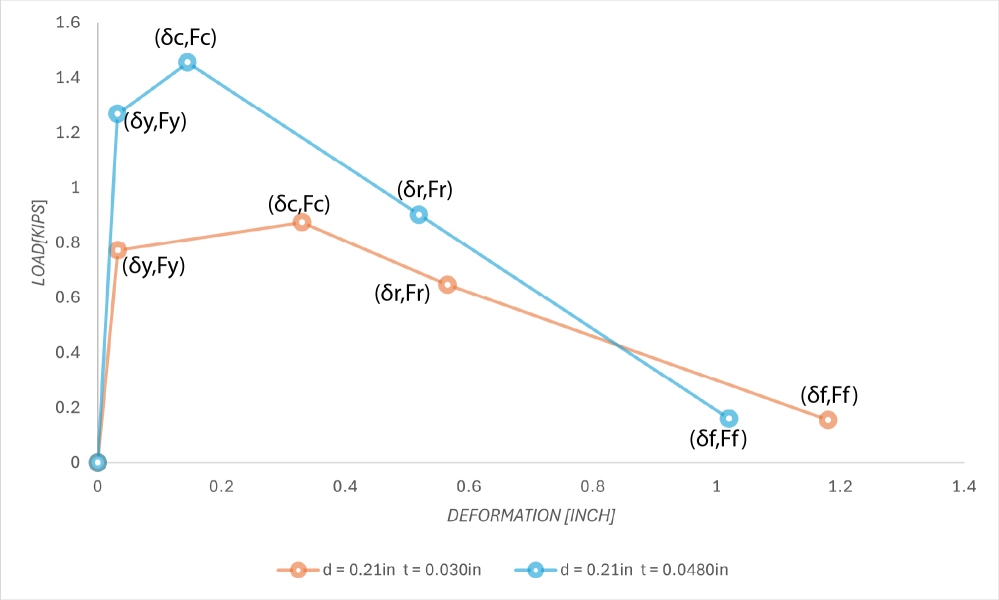

Figure 2: Load-deformation relationship of Screw

diaphragm response. Two examples of monotonic screw backbone curves used in this study are shown in Figure 2, illustrating the progression from initial elastic behavior through peak strength, followed by gradual post-peak softening and residual response.

2.1.2 Arc Spot Welds

The load–deformation characteristics of arc spot welds were derived from Snow and Easterling (2008), which performed a series of lap-shear tests on welds fabricated with nominal visual diameters of 5/8 in (16 mm) and 3/4 in (19 mm). They investigated various combinations of sheet thicknesses ranging from 22-ga (0.7 mm) to 16-ga (1.6 mm), single and double sheet layers, and different welding times (full, 2/3, and 1/3). Two primary failure modes were identified in the tests: weld failure (WF) and sheet tearing (ST). Because the ICM evaluates diaphragm strength through the nonlinear shear response of the connectors, only load–deformation curves associated with weld failure were utilized. Specimens governed by sheet tearing were excluded, as these represent sheet limit states rather than fastener-controlled behavior. This filtering ensures that the load–deformation data used in the ICM directly reflect the mechanical behavior of the fastener system responsible for carrying shear.

For each candidate diaphragm selected from SDI DDM (Luttrell 2006) and SDII database (O'Brien 2017), the corresponding weld load–deformation curve was identified directly from the Snow and Easterling data set based on the actual diameter and sheet thickness of the weld used in the corresponding diaphragm specimen. The documented combinations between weld size, deck thickness, and failure mode reported by Snow and Easterling (2008) were used to confirm consistent weld failure behavior across repeated trials. Only cases that exhibited weld failure in all replicate tests under monotonic loading were selected. The corresponding load–deformation curves for those parameter combinations were then digitized directly using WebPlotDigitizer (Rohatgi (2014)) and applied in the ICM framework without modification or curve fitting.

This approach provides a more realistic representation of weld behavior compared to the simplified trilinear model previously employed by Koh et al. (2025) which did not fully capture the softening response observed in experimental welds. Moreover, by incorporating the measured nonlinear deformation of welds and restricting the dataset to confirmed weld failures, the present model more accurately reflects the true fastener behavior under shear loading. For diaphragm thicknesses not exactly matching those in Snow and Easterling (2008), weld data were rounded to the nearest available gauge to ensure the most representative correlation between experimental and analytical specimens.

2.2 Strength Estimation Using the Instantaneous Center Method

To evaluate the deformation demand on each fastener for a given diaphragm configuration, an initial estimate of the instantaneous center of rotation (IC) is first assigned. The initial IC location is taken at the geometric centroid of the fastener group, where the coordinate system shown in Figure 1 defines the positive x–y directions. For a trial IC position, the fastener located farthest from the IC experiences the maximum deformation $\delta_{\max}$, determined from the applicable load deformation curves. The deformation of the k-th fastener δ_k is then scaled relative to its radial distance from the IC as shown in Eq. 2:

$$\delta_k = \frac{r_k}{r_{\max}} \delta_{\max} \tag{2}$$

where $r_{\max}$ is the distance from the IC to the farthest fastener, and r_k is the distance from the IC to the k-th fastener.

Each fastener develops a resisting force R_k based on its deformation demand and the corresponding monotonic backbone curve. Using the connection geometry, the horizontal and vertical components of R_k are computed as shown in Eq. 3 and Eq. 4:

$$(R_k)_x = -\frac{dy}{d}\frac{R_k}{R_{ult}} R_{ult} \tag{3}$$

$$(R_k)_y = \frac{dx}{d}\frac{R_k}{R_{ult}} R_{ult} \tag{4}$$

The combined forces contributed by all fasteners must satisfy the equilibrium equations for a planar system as given in Eq. 5:

$$P_x + \sum (R_k)_x = 0, \qquad P_y + \sum (R_k)_y = 0, \qquad \sum M = 0 \tag{5}$$

where P_x and P_y are the x and y components of the applied unit load, repectively, and $\sum M$ represents moment equilibrium about a chosen reference point. If these conditions are not met, a new IC location is selected and the procedure is repeated. The iterative search continues until equilibrium is satisfied within a tolerance of 0.001. Once the IC converges, the corresponding value of the applied unit load P represents the predicted ultimate strength of the diaphragm.

3. Results

This section compares diaphragm strengths predicted by the ICM with three sources: (1) experimental results from the Steel Deck Institute (SDI) Diaphragm Design Manual (Luttrell 2006), (2) experimental results from the Steel Diaphragm Innovation Initiative (SDII) database curated by O'Brien (2017), and (3) estimates based on the diaphragm shear strength provisions in Section D of AISI S310-16 (2016), which are based on elastic analysis.

3.1 Steel Deck Institute Diaphragm Design Manual (SDI DDM)

Welded diaphragm specimens were selected from two specimen series reported in the Steel Deck Institute (SDI) Diaphragm Design Manual (Luttrell 2006): the WB-series, which corresponds to a wide-rib deck profile, and the I-series, which corresponds to an intermediate-rib deck profile. Both specimen sets only utilize welded support fasteners without side-lap screws, which allows the diaphragm response to be governed solely by the behavior of the arc-spot welds. The general layout of the welds is illustrated in Fig. 1. The differences in deck profiles are shown in Fig. 3, and the corresponding geometric dimensions are summarized in Table 1. Incorporating both deck types enables the ICM with refined fastener load–deformation curves to be evaluated across specimens with varying cross-sections and weld locations relative to the rib geometry.

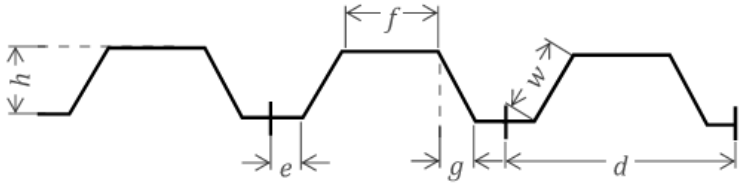

Figure 3: Cross-sectional deck profiles for the welded specimens

All specimens selected from the SDI DDM used 5/8 in. (15.9 mm) diameter arc spot welds. To model weld behavior, this study adopted thickness-specific monotonic weld-failure backbone curves from Snow and Easterling (2008), corresponding to sheet thicknesses available in the literature: 16-ga, 18-ga, 20-ga, and 22-ga. Rather than treating the WB- and I-series as separate groups, all welded specimens were organized according to these gauge categories so that each specimen could be assigned the weld backbone curve most representative of its tested thickness and weld diameter. This thickness-based grouping aligns directly with the way weld load-deformation relationships are defined, providing a consistent basis for evaluating the predictive performance of the ICM model with refined load-deformation curves across different deck geometries.

Table 1: Deck profile dimensions for WB- and I-series specimens

Deck Type	f (in.)	e (in.)	g (in.)	w (in.)	d (in.)
Wide Rib Deck (WB)	3.75	1.00	0.125	1.5052	6.00
Intermediate Rib Deck (I)	4.50	0.625	0.125	1.5052	6.00

3.1.1 Results for 22-gauge Specimens (22-ga)

The 22-ga group includes welded diaphragm specimens from the WB-series and I-series whose tested sheet thicknesses fall within this gauge category. All specimens in this group were evaluated using the 22-ga weld-failure (WF) backbone curve from Snow and Easterling (2008). Table 2 summarizes the experimental strengths, AISI predictions, and the corresponding strengths predicted by the Instantaneous Center Method (ICM) with refined fastener load–deformation curves. From Table 2, the ICM model with refined fastener load–deformation curves shows an average

Table 2: Comparison of experimental, AISI, and ICM strengths for 22-ga specimens

Specimen	w (ft)	L (ft)	L_s (ft)	t (in)	S_u (klf)	Strength ratio		
						ICM/Exp	AISI/Exp	ICM/AISI
WB-7	16	20	6.67	0.0323	0.307	0.604	0.624	0.969
WB-8	16	20	4.00	0.0314	0.524	0.866	0.852	1.017
WB-9	16	20	4.00	0.0283	0.558	1.259	1.319	0.955
WB-10	16	20	6.67	0.0270	0.267	0.956	0.859	1.114
WB-11	16	20	6.67	0.0270	0.267	0.877	0.788	1.114
I-5	16	20	5.00	0.0284	0.386	1.354	1.225	1.105
I-6	16	20	6.67	0.0284	0.288	1.081	1.047	1.032
					Average	1.000	0.959	1.044

ICM-to-experimental strength ratio of approximately 1.00, indicating that the ICM model prediction for this group is almost similar to the experimentally measured diaphragm strengths. The corresponding AISI-to-experimental average of 0.96 reflects the conservative nature of the elastic AISI method, while the average ICM/AISI ratio of 1.04 confirms that the ICM with refined fastener load–deformation curves generally predicts higher strengths than the elastic approach. Although individual specimens exhibit some scatter, the overall trends demonstrate that the ICM with refined fastener load–deformation curves provides consistent strength predictions for 22-ga welded diaphragm specimens.

3.1.2 Results for 20-gauge Specimens (20-ga)

The 20-ga group includes welded diaphragm specimens from the WB-series and I-series whose tested sheet thicknesses fall within this gauge category. All specimens in this group were evaluated using the 20-ga weld-failure (WF) backbone curve from Snow and Easterling (2008). Table 3 summarizes the experimental strengths, AISI predictions, and the corresponding strengths predicted by the refined Instantaneous Center Method (ICM).

From Table 3, the ICM with refined fastener load–deformation curves model provides generally good predictions for the 20-ga specimens. The average ICM-to-experimental strength ratio is 0.83, indicating that the model remains conservative on average while capturing the overall diaphragm strength with reasonable accuracy. The corresponding AISI-to-Experimental average of 0.794 shows that the elastic AISI method is slightly more conservative than the ICM-to-Experimental as expected. The average ICM/AISI ratio of 1.06 confirms that the ICM with refined fastener

Table 3: Comparison of experimental, AISI, and ICM strengths for 20-ga specimens

Specimen	w (ft)	L (ft)	L_s (ft)	t (in)	Strength (kip/ft)	Strength ratio		
						ICM/Exp	AISI/Exp	ICM/AISI
WB-3	16	20	6.67	0.0365	0.401	0.711	0.835	0.851
WB-4	16	20	4.00	0.0365	0.665	0.774	0.858	0.903
WB-5	16	20	5.00	0.0351	0.440	0.885	0.838	1.056
WB-6	16	20	5.00	0.0353	0.398	0.801	0.686	1.167
WB-14	16	16	5.33	0.0365	0.524	0.745	0.729	1.022
WB-15	16	16	5.33	0.0365	0.524	0.703	0.755	0.931
WB-16	16	12	6.00	0.0365	0.491	1.030	0.986	1.045
WB-17	16	20	6.67	0.0365	0.458	1.094	0.790	1.385
WB-18	16	16	5.33	0.0365	0.595	0.875	0.657	1.333
WB-37	16	20	6.67	0.0365	0.401	0.834	0.980	0.851
WB-40	16	20	5.00	0.0365	0.541	0.667	0.777	0.859
WB-41	16	12	6.67	0.0365	0.491	0.880	0.842	1.045
I-1	16	20	10.0	0.0343	0.192	0.639	0.549	1.164
I-4	16	20	5.00	0.0345	0.423	0.868	0.791	1.098
I-7	16	20	6.67	0.0342	0.300	0.948	0.833	1.137
					Average	0.830	0.794	1.056

load–deformation curves consistently predicts higher strengths than the elastic AISI approach, as expected for an inelastic analysis. Although several individual specimens exhibit moderate scatter, including a small number of ICM/Exp ratios slightly greater than unity, the overall trends indicate that the ICM with refined fastener load–deformation curves provides an improved prediction of diaphragm strength for 20-ga welded specimens.

3.1.3 Results for 18-gauge Specimens (18-ga)

The 18-ga group includes welded diaphragm specimens from the WB-series and I-series whose tested sheet thicknesses fall within this gauge category. All specimens in this group were evaluated using the 18-ga weld-failure (WF) backbone curve from Snow and Easterling (2008). Table 4 summarizes the experimental strengths, AISI predictions, and the corresponding strengths predicted by the refined Instantaneous Center Method (ICM).

From Table 3, the ICM model provides good predictions for most of the 18-ga specimens. For WB-1 and WB-13 in the WB-series, and for both I-series specimens (I-2 and I-3), the ICM strengths fall between the experimental and AISI values, which reflects the expected trend of an inelastic model predicting higher strength than AISI but remaining below the experimental capacity. One notable observation is WB-38, whose experimental values are lower than AISI predicted strength values, which leads the ICM with refined fastener load–deformation curves to overpredict its capacity. Overall, the ICM demonstrates strong predictive performance for the 18-ga group, with consistent

Table 4: Comparison of experimental, AISI, and ICM strengths for 18-ga specimens

Specimen	w (ft)	L (ft)	L_s (ft)	t (in)	Strength (kip/ft)	Strength ratio		
						ICM/Exp	AISI/Exp	ICM/AISI
WB-1	16	20	5.00	0.0505	0.803	0.773	0.637	1.212
WB-13	16	16	5.33	0.0496	0.780	0.868	0.693	1.252
WB-38	16	20	6.67	0.0496	0.599	1.664	1.302	1.278
I-2	16	20	10.0	0.0469	0.413	0.890	0.751	1.180
I-3	16	20	6.67	0.0444	0.500	0.910	0.662	1.380
					Average	1.021	0.809	1.260

trends across four of the five specimens.

3.1.4 Results for 16-gauge Specimens (16-ga)

The 16-ga group includes welded diaphragm specimens from the WB-series whose tested sheet thicknesses fall within this gauge category. All specimens in this group were evaluated using the 16-ga weld-failure (WF) backbone curve from Snow and Easterling (2008). Table 5 summarizes the comparisons of the experimental strengths, AISI predictions, and the ICM predictions.

Table 5: Comparison of experimental, AISI, and ICM strengths for 16-ga specimens

Specimen	w (ft)	L (ft)	L_s (ft)	t (in)	Strength (kip/ft)	Strength ratio		
						ICM/Exp	AISI/Exp	ICM/AISI
WB-12	16	16	5.33	0.0587	1.046	0.601	0.663	0.910
WB-39	16	20	8.66	0.0587	0.754	1.020	1.022	0.998
					Average	0.811	0.842	0.953

From Table 5, it can be seen that specimen WB-12 exhibits a relatively high experimental strength compared to the ICM and AISI predictions, resulting in conservative estimates for both methods. In contrast, specimen WB-39 exhibits a slightly lower experimental strength, resulting in both predictions producing mild overpredictions. Notably, the AISI/Exp ratio for WB-39 is greater than 1.0, which is uncommon because the elastic AISI method typically provides a conservative lower-bound estimate of diaphragm strength. Overall, the ICM with refined fastener load–deformation curves model demonstrates reasonable accuracy for the 16-ga group, with its average strength ratio falling between the corresponding AISI average and the experimental results.

3.2 Steel Diaphragm Innovation Initiative Database

The Steel Diaphragm Innovation Initiative (SDII) database (O'Brien 2017) contains experimental diaphragm test results obtained under both monotonic and cyclic loading conditions. From this database, diaphragm specimens subjected to monotonic loading were selected for comparison with the ICM proposed in this study. The selected specimens include tests reported by Pinkham (1999) and Essa et al. (2003), covering deck thicknesses ranging from 0.028 to 0.059 in. (0.7 to 1.5 mm).

Unlike the WB- and I-series specimens selected from the SDI Diaphragm Design Manual, the SDII specimens incorporate both welded support fasteners and screwed side-lap fasteners. Arc spot welds were used for edge, end, and interior support fasteners, while screws were used at the side-lap locations (Figure. 1).

Table 6: SDII specimens and comparison results

Specimen	w (ft)	L (ft)	L_s (ft)	t (in)	Strength	Strength ratio		
					(kip/ft)	ICM/Exp	AISI/Exp	ICM/AISI
Pinkham (1999)								
50	15	15	5	0.048	5.17	0.894	0.835	1.071
51	15	15	5	0.031	3.38	1.452	1.127	1.289
52	21	20	10	0.031	1.30	1.740	1.367	1.273
53	21	20	10	0.031	1.98	1.193	1.253	0.952
54	21	20	10	0.048	2.24	0.872	1.179	0.740
Essa et al. (2003)								
11	12	20	5	0.030	0.917	1.618	0.746	2.170
15	12	20	5	0.030	1.540	1.531	1.185	1.292
					Average	1.329	1.099	1.255

Note: Exp = experimental results.

From Table 6, the ICM predictions were compared with the experimental results for the SDII specimens incorporating mixed fastener systems. The combined average ICM-to-experimental strength ratio is 1.33, indicating an overall tendency for the ICM to overpredict diaphragm strength for this dataset. The corresponding AISI-to-experimental average of 1.10 shows that the elastic AISI method also overpredicts strength on average. In particular, several Pinkham specimens (51, 52, 53, and 54) exhibit AISI-to-experimental ratios greater than 1.0, indicating that even the elastic design approach predicts strengths exceeding the measured experimental values. Similar behavior is observed for the Essa specimen 15, for which the elastic AISI prediction exceeds the experimental strength. Because the ICM is formulated as an inelastic analysis, it is expected to produce strength predictions that exceed those of the elastic AISI method, resulting in a slightly larger difference relative to the experimental results for these specimens. This observed over-prediction is more pronounced for specimens with thinner deck sections and mixed fastener configurations, highlighting the increased sensitivity of diaphragm strength predictions to the assumed fastener load–deformation behavior when both arc spot welds and side-lap screws are present.

4. Discussion

From Section 3, it was observed that the assumed fastener load–deformation behavior strongly influences the ICM predictive performance. By replacing the generalized fastener relationship used in Koh et al. (2025) with thickness-dependent weld and screw load deformation backbone curves, the ICM with refined load-deformation relationships presented in this study demonstrated

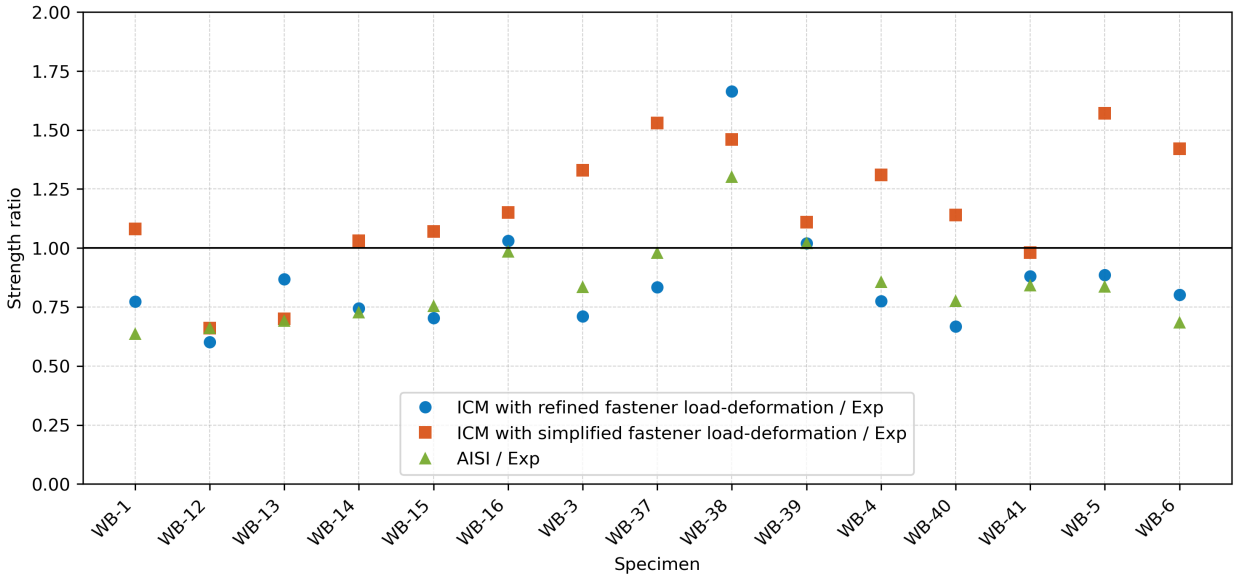

Figure 4: Comparison of strength ratios predicted using the ICM with refined fastener load–deformation curves, the ICM with generalized fastener load-deformation curves, and the elastic AISI method for selected WB-series SDI DDM specimens.

improved agreement with experimental results for steel deck diaphragms across a range of deck gauges. As illustrated in Figure 4, this improvement is most pronounced for diaphragms constructed with thicker deck profiles, where fastener behavior plays a dominant role in governing diaphragm strength. For several 16- and 18-ga specimens (e.g., WB-1, WB-13 and WB-39), the ICM with refined fastener load–deformation curves produces strength ratios that lie closer to 1.0 than those predicted by either the elastic AISI method or the ICM with simplified load-deformation relationships, indicating closer agreement with experimental behavior. In these thicker diaphragms, elastic methods tend to be overly conservative. By explicitly accounting for thickness-dependent fastener response, the ICM with refined fastener load–deformation curves captures a more realistic balance between stiffness degradation and force redistribution. Collectively, these observations suggest that the ICM with refined fastener load–deformation curves is particularly well suited for evaluating thicker steel deck diaphragms (e.g., 16–18-ga), where fastener-controlled inelastic behavior governs response and elastic assumptions are more conservative.

5. Conclusions

This study advances the application of the Instantaneous Center Method (ICM) for estimating the shear strength of bare steel deck diaphragms by refining the modeling of fastener load–deformation behavior. Building on the ICM framework established by Koh et al. (2025), which incorporated simplified and generalized fastener response models, this paper aims to improve predictive accuracy by directly using thickness- and geometry-specific backbone curves for arc-spot welds and sheet-to-sheet screws. Rather than employing generalized fasteners' load-deformation relationships derived from experimental trends, the refined approach in this study associates experimentally derived backbone curves with the fastener geometries and sheet thicknesses used in each analyzed diaphragm specimen.

Comparisons of ICM-predicted diaphragm strengths with experimental results and elastic design provisions demonstrated that the refined fastener models significantly reduce the overestimation observed in prior ICM implementations that did not consider explicit effects of fastener geometry and sheet thickness. By better representing nonlinear stiffness degradation and post-peak behavior at the fastener level, the ICM with refined fastener load–deformation curves more accurately captured the force redistribution within fastener groups that govern diaphragm response. The results confirmed that the previously observed differences were driven by simplifications in fastener modeling, particularly for arc-spot welds, where the strength and deformation response are sensitive to sheet thickness and effective weld diameter. Furthermore, the study confirmed the applicability of the ICM to diaphragms incorporating different fastener types within a unified analysis framework, including configurations with arc-spot welds only as well as diaphragms with both welds and side lap screws. These findings strengthen the case for using the ICM as a mechanics-based alternative to elastic diaphragm design methods when appropriate fastener load–deformation models are available.

While the proposed ICM approach improved strength prediction accuracy, additional work remains to fully generalize the method for use of this approach in practice. Future research should focus on expanding experimentally derived fastener databases to include additional weld diameters, sheet thickness combinations, and fastener types, as well as further validation against a broader range of diaphragm configurations. Continued investigation into diaphragm flexibility and its interaction with the rigid-body rotation assumption inherent in the ICM may also lead to further improvements in predictive capability. However, the results of this study demonstrate that the careful data-driven refinement of the fastener modeling substantially enhances the reliability of ICM-based diaphragm strength predictions and represents a significant step toward a practical nonlinear analysis of steel deck diaphragms. From a stability perspective, the results indicate that diaphragm limit states may be governed by fastener-level stiffness degradation, which can lead to loss of equilibrium within the fastener group prior to reaching elastic strength limits. By more accurately representing nonlinear fastener behavior, the ICM framework, incorporating refined fastener load-deformation models, provides improved insight into stability-related response mechanisms associated with fastener-controlled diaphragm behavior.

References

AISI S100-16 (2016). *North American Specification for the Design of Cold-Formed Steel Structural Members*. American Iron and Steel Institute.

AISI S310-16 (2016). *North American Specification for the Design of Profiled Steel Diaphragms Panels*. American Iron and Steel Institute.

Brandt, G Donald (1982). "Rapid determination of ultimate strength of eccentrically loaded bolt groups". In: *Engineering Journal* 19.2, pp. 94–100.

Crawford, Sherwood F and Geoffrey L Kulak (1971). "Eccentrically loaded bolted connections". In: *Journal of the Structural Division* 97.3, pp. 765–783. DOI: 10.1061/JSDEAG.0002844.

Derveni, Fani, Simos Gerasimidis, and Kara D Peterman (2020). "Nonlinear fastener-based modeling of cold-formed steel shear walls". In: *Structures Congress 2020*. American Society of Civil Engineers Reston, VA, pp. 697–708.

Essa, Hesham S, Robert Tremblay, and Colin A Rogers (2003). "Behavior of roof deck diaphragms under quasistatic cyclic loading". In: *Journal of Structural Engineering* 129.12, pp. 1658–1666.

Kalo, Rita and Kara Peterman (2020). "Stiffness Characterization of Single Lap Shear Screw-Fastened Connections Using Finite Element Modeling". In: *Proceedings of the Cold-Formed Steel Research Consortium (CFSRC) Colloquium*. Cold-Formed Steel Research Consortium. Baltimore, MD. URL: https://jscholarship.library.jhu.edu/server/api/core/bitstreams/444f8d19-734e-4fd9-96a5-5d82da9979f7/content.

Koh, Hyeyoung, Thomas Sputo, and Hannah B Blum (2025). "Inelastic Analysis of Bare Steel Deck Diaphragms Using the Instantaneous Center Method". In: *Journal of Structural Design and Construction Practice* 30.2, p. 06025002.

Luttrell, Larry D (2006). *Steel Deck Institute Diaphragm Design Manual*. Steel Deck Institute.

Moen, CD et al. (2014). "Towards load-deformation models for screw-fastened cold-formed steel-to-steel shear connections". In: *International Specialty Conference on Cold-Formed Steel Structures*.

O'Brien, Patrick Emmet (2017). "Characterizing the load-deformation behavior of steel deck diaphragms using past test data". PhD thesis. Blacksburg, VA: Virginia Tech.

Pinkham, C. (1999). "Data from testing of Wheeling High Strength Decking". Personal communication from Jeff Martin, Verco Manufacturing; data obtained March 2017.

Rohatgi, Ankit (2014). *WebPlotDigitizer User Manual*. Version 3.4, pp. 1–18. URL: https://automeris.io/WebPlotDigitizer/app.

Snow, Gregory L and W Samuel Easterling (2008). *Strength of arc spot welds made in single and multiple steel sheets*. Tech. rep. CE/VPI-ST-08/02. Blacksburg, VA: Virginia Polytechnic Institute and State University.

Tao, Fannie, A Chatterjee, and CD Moen (2016). "Monotonic and cyclic response of single shear cold-formed steel-to-steel and sheathing-to-steel connections". In: *Virginia Tech Research Report No. CE/VPI-ST-16/01, Blacksburg, VA, USA*.

Torabian, S and BW Schafer (2021). "Cyclic experiments on sidelap and structural connectors in steel deck diaphragms". In: *Journal of structural engineering* 147.4, p. 04021028.